

Effect of pressure on the low-temperature exciton absorption in GaAs

A. R. Goñi, A. Cantarero,* K. Syassen, and M. Cardona

*Max-Planck-Institut für Festkörperforschung, Heisenbergstrasse 1, Postfach 80 06 65,
D-7000 Stuttgart 80, Federal Republic of Germany*

(Received 30 November 1989)

We have measured low-temperature exciton optical-absorption spectra at the lowest direct band edge (E_0) of GaAs as a function of pressure up to 9 GPa. Spectra are analyzed in terms of the Elliott model by taking into account the broadening of the exciton line. In this way, we determine the dependence on pressure of the E_0 gap, the exciton binding energy \mathcal{R} , and exciton linewidth at different temperatures. The pressure coefficient of the E_0 fundamental gap [107(4) meV/GPa] is found to be independent of temperature. The exciton binding energy increases with pressure at a rate of $d \ln \mathcal{R} / dP = 0.083(3) \text{ GPa}^{-1}$. The exciton lifetime becomes smaller for pressures above the crossover between Γ - and X -point conduction-band minima ($P > 4.2 \text{ GPa}$), a fact which is attributed to phonon-assisted intervalley scattering. From the pressure dependence of the exciton linewidth we determine an accurate value for the intervalley deformation-potential constant $D_{\Gamma X} = 4.8(3) \text{ eV/\AA}$.

I. INTRODUCTION

The effect of exciton formation on the optical absorption of tetrahedral semiconductors near the direct band edge is well established through a large body of experimental¹⁻⁵ and theoretical^{4,6-9} investigations. Direct optical transitions into discrete exciton states give rise to a hydrogenlike series of absorption lines for photon energies just below the bandgap, and transitions to the exciton continuum cause an enhancement of the absorption above the gap energy.¹⁰ The exciton binding energy (\mathcal{R}) typically is a few meV [$\mathcal{R} = 4.2(1) \text{ meV}$ for GaAs (Ref. 1)]. In high-quality crystals the exciton linewidth is primarily determined by electron-phonon scattering. Thus, in optical-absorption exciton lines of tetrahedral semiconductors are well resolved only at low temperatures.¹¹

The effect of pressure on excitonic optical absorption has been investigated at room temperature for a number of semiconductors with strong-excitonic features for which the exciton binding energy is about 1 order of magnitude larger than typical values for III-V compounds. Among these are Cu halogenides¹² and layered materials like GaSe or InSe.¹³⁻¹⁵ More recently, the exciton luminescence of Cu_2O under pressure¹⁶ was measured at low temperatures. One of the main aspects in these previous pressure studies of excitonic effects in semiconductors was to determine the shift of band gaps or change of excitonic binding energies under compression.

In this work we report the effect of hydrostatic pressure ($P < 9 \text{ GPa}$) on the excitonic band-edge absorption of GaAs at low temperatures. The pressure-dependent optical-absorption spectra are analyzed in terms of a modified Elliott model,¹⁰ which takes into account the finite exciton lifetime. We determine the pressure coefficients of the band gap E_0 and exciton binding energy \mathcal{R} at different temperatures. Furthermore, we obtain

the pressure dependence of the exciton linewidth. The latter aspect is of particular interest because GaAs, which is a direct-band-gap semiconductor at ambient pressure, becomes an indirect-band-gap material for $P_c > 4.2 \text{ GPa}$.¹⁷ We find a pronounced broadening of the exciton line above the Γ - X crossover, which increases with energy separation between Γ - and X -point conduction-band minima. This behavior is attributed to phonon-assisted scattering of excited electrons from the Γ - to the X -point conduction-band valleys. From the pressure-induced broadening of the exciton optical-absorption peak we derive a reliable value for the phonon deformation-potential constant for Γ - X intervalley scattering in GaAs. A preliminary account of this work has been published in Ref. 18.

II. EXPERIMENTAL DETAILS AND SPECTRA

Transitions from the top of the valence band at point Γ to s -like exciton states are dipole allowed, and the corresponding absorption coefficient is quite large¹⁹ ($\alpha \sim 10^4 \text{ cm}^{-1}$). Therefore very thin samples are needed for exciton optical-absorption measurements. The samples investigated here ($\sim 100 \times 100 \mu\text{m}^2$ size) were cut from a bulk semi-insulating GaAs wafer, which was mechanically polished down to a final thickness of $\sim 4 \mu\text{m}$. Optical-absorption measurements were performed at 200, 100, and 20 K by using a diamond-window high-pressure cell [diamond anvil cell (DAC)] in combination with a flow-cryostat and a micro-optical system. Because of the sensitivity of the exciton optical-absorption peak to uniaxial-stress components,¹¹ condensed helium was used as a pressure-transmitting medium. In this way we ensure the best possible hydrostatic conditions also at low temperatures. The pressure was measured *in situ* using the ruby fluorescence method.^{20,21} At a given temperature, a pressure-independent wavelength offset of the

ruby luminescence is taken into account,²² and the calibration of the pressure scale is thus assumed to be independent of temperature.²³

For absorption measurements white light from a tungsten lamp was focused onto the sample, forming a light spot of $\sim 60 \mu\text{m}$ in diameter. The transmitted light was then passed through a $\frac{3}{4}$ -m single-grating monochromator and detected by a cooled GaAs photomultiplier coupled to a fast photon-counting system. The absorption coefficient $\alpha(\omega)$ was determined according to

$$\alpha(\omega) = \frac{1}{d} \ln \left[\frac{I_0(\omega)}{I(\omega)} \right] - \alpha_c, \quad (1)$$

where $I(\omega)$ and $I_0(\omega)$ are the intensity transmitted through the sample and the reference intensity measured with light passing through the pressure cell next to the sample, respectively. The sample thickness d was determined from interferences in transmitted light at photon energies below the absorption edge. The quantity α_c takes into account reflection losses at sample and diamond window surfaces. For each pressure and temperature two spectra were recorded: one in a wide spectral range of energies from far below to well above the absorption edge, the second one was taken with higher resolution (0.2 meV) in the energy range close to the exciton line. All absorption spectra measured in the wide range of energies were rescaled to a common value of $\alpha=0$ at $\hbar\omega=1.4$ eV, where GaAs is transparent. These spectra were used as a reference for the absorption spectra in the direct exciton region. In this way it was possible to determine the correction term α_c and thus absolute values for the absorption coefficient in the excitonic region.

Figure 1 shows some representative optical-density spectra of GaAs at 100 K measured at different pressures in an extended spectral range around the direct band gap. High-resolution spectra of the absorption edge at different temperatures and pressures are shown in Fig. 2. The peak at the absorption edge is assigned to optical

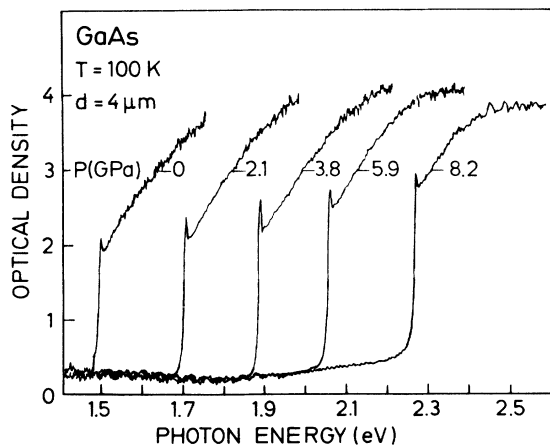


FIG. 1. Absorption spectra of a thin GaAs sample near the direct band gap measured for different pressures at $T=100$ K.

transitions into discrete exciton states dominated by that with principal quantum number $n=1$. Individual absorption lines corresponding to $n>1$ exciton levels,¹ which should be 1 order of magnitude weaker than the $n=1$ line, could not be resolved for the samples used here presumably because of residual line broadening due to impurity scattering. The decrease of the exciton linewidth with decreasing temperature reveals a significant contribution of phonon-scattering processes to the lifetime. With increasing pressure the exciton peak shifts towards higher energies, following the blue shift of the E_0 band gap with pressure.¹⁷ As the pressure increases to about 4 GPa the exciton peak becomes more pronounced. Above ~ 4.2 GPa, where the Γ - X crossover in GaAs occurs,¹⁷ the exciton starts to broaden monoton-

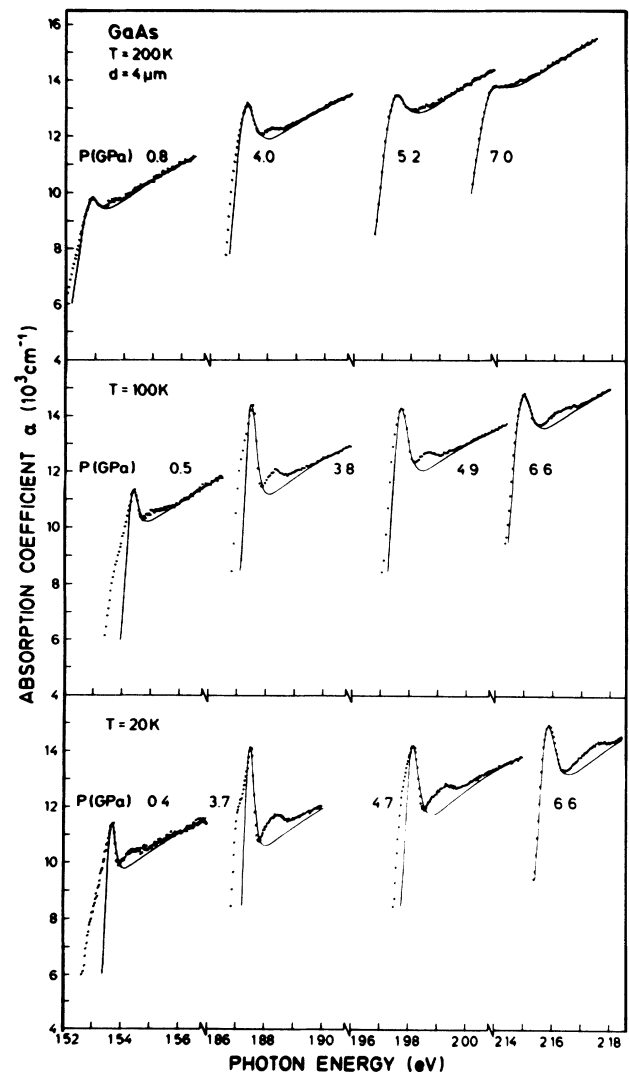


FIG. 2. Exciton-absorption spectra (data points) of GaAs near the direct gap E_0 at different pressures and at 200, 100, and 20 K. Solid lines represent fits to the experimental data with Eq. (7).

ically. This line-broadening effect is stronger at higher temperatures; for example, at 7 GPa and 200 K the excitonic peak is not well defined anymore. The line broadening is attributed to electronic intervalley scattering into X conduction-band states that are assisted by zone-edge phonons.

III. ANALYSIS AND DISCUSSION

A. Model for the exciton line shape

The hydrogenlike bound exciton states ($1s, 2s, \dots$) arising from Coulomb interaction between electrons and holes are characterized by the effective Rydberg energy \mathcal{R} and Bohr radius a_B :¹⁰

$$\mathcal{R} = \frac{\mu e^4}{2\hbar^2 \epsilon^2}, \quad a_B = \frac{\epsilon \hbar^2}{\mu e^2}. \quad (2)$$

Here, μ is the exciton-reduced mass and ϵ the low-frequency dielectric constant. Equation (2) applies to the case of direct allowed interband transitions between non-degenerate parabolic bands. Excitonic states are broadened through exciton-phonon interaction giving rise, in the weak exciton-phonon coupling limit, to a Lorentzian line shape.²⁴ A finite linewidth of the exciton states can be introduced in the Elliott expression for the absorption coefficient¹⁰ by means of a Lorentzian convolution function. The absorption coefficient then takes the form²⁵

$$\alpha(\hbar\omega) = \frac{2\pi\mathcal{R}^{1/2}(2\mu)^{3/2}e^2}{n(\omega)c\hbar^2m_0} f_{cv} \left[\sum_{m=1}^{\infty} \frac{2\mathcal{R}}{m^3} \frac{\Gamma_m}{(\hbar\omega - E_m)^2 + \Gamma_m^2} + \int_{E_0}^{\infty} dE \frac{1}{1 - e^{-2\pi z}} \frac{\Gamma_c}{(\hbar\omega - E)^2 + \Gamma_c^2} \right] \quad (3a)$$

with

$$z^2 = \mathcal{R}/(E - E_0); \quad E_m = E_0 - \mathcal{R}/m^2, \quad m = 1, 2, \dots; \quad (3b)$$

here, m_0 is the free electron mass, c the speed of light, $n(\omega)$ the refractive index, and f_{cv} the oscillator strength for optical transitions between valence and conduction bands. Within the dipole approximation f_{cv} is given by

$$f_{cv} = 2|M_R|^2/(m_0\hbar\omega), \quad (4)$$

where M_R is the matrix element for electron-photon interaction. We simplify Eq. (3) by defining the absorption-strength parameter

$$C_0 = \frac{4\pi(2\mu)^{3/2}e^2|M_R|^2}{nc\hbar^2m_0^2}. \quad (5)$$

$$\alpha(\hbar\omega) = \frac{C_0\mathcal{R}^{1/2}}{\hbar\omega} \left\{ \sum_{n=1}^{\infty} \frac{2\mathcal{R}}{m^3} \frac{\Gamma_m}{(\hbar\omega - E_m)^2 + \Gamma_m^2} + \frac{1}{2} \left[\frac{\pi}{2} - \arctan \left(\frac{\hbar\omega - E_0}{\Gamma_c} \right) \right] - \sum_{m=1}^{\infty} \frac{\mathcal{R}}{m^3} \frac{\Gamma_c}{(\hbar\omega - E_m)^2 + \Gamma_c^2} + \frac{\pi}{2} \frac{\sinh(2u^+)}{\cosh(2u^+) - \cos(2u^-)} \right\} \quad (7a)$$

with

$$u^{\pm} = \pi(\mathcal{R}/2)^{1/2} \left[\frac{[(\hbar\omega - E_0)^2 + \Gamma_c^2]^{1/2} \pm (\hbar\omega - E_0)}{(\hbar\omega - E_0)^2 + \Gamma_c^2} \right]^{1/2}. \quad (7b)$$

Because of the $1/m^3$ factor in the summation, terms with $m > 3$ can be neglected.

Equation (7) describes the spectral dependence of the absorption coefficient near the direct exciton transition. This analytical form is used here for the analysis of the experimental absorption spectra. Figure 3 illustrates the result of a fit of Eq. (7) to the absorption data of GaAs at 6.1 GPa and 100 K. The fitting parameters are E_{1s} (the

For the linewidth of the m th line we use the empirical relation²⁶

$$\Gamma_m = \Gamma_c - (\Gamma_c - \Gamma_1)/m^2, \quad (6)$$

with the linewidth Γ_1 and Γ_c of the $m=1$ state and of the continuum, respectively.

The integral in Eq. (3) represents the contribution of the exciton continuum to the absorption coefficient. It can be separated into two parts: the first one gives an arctan function, while the second can be solved by integration in the complex plane (see the Appendix for details). In this way we obtain the following analytical expression:

energy position of the $m=1$ exciton line), \mathcal{R} , Γ_1 , Γ_c , and C_0 . The different contributions to $\alpha(\omega)$ are also shown separately in Fig. 3. Curve I represents the total contribution of the discrete exciton spectrum. The superposition of the discrete absorption lines, weighted by the factor $1/m^3$, yields a single peak roughly centered at the energy E_{1s} , and approximately of width Γ_1 . The curves labeled II and III in Fig. 3 represent the exciton continuum and correspond to the second term and the sum of the third and fourth terms in Eq. (7), respectively, which together yield a steplike absorption edge of width Γ_c .

The solid lines in Fig. 2 represent the results of non-linear least-squares fits to absorption spectra of GaAs measured at other pressures and temperatures. The main

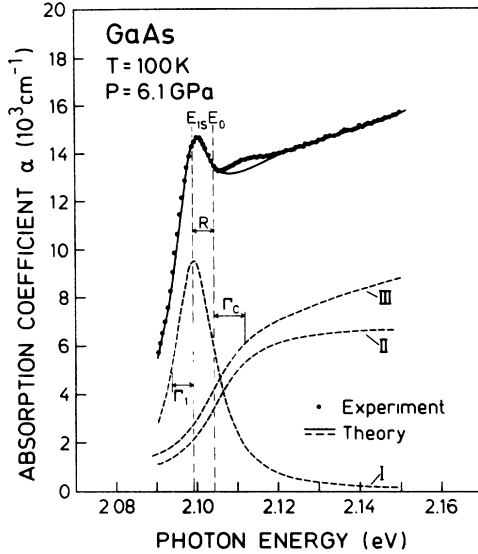


FIG. 3. Exciton-absorption spectrum of GaAs at 6.1 GPa and 100 K. The solid line represents the result of fitting the model function (7) to the experimental data. Dashed lines correspond to contributions of individual terms in Eq. (7) to the absorption (see text for details).

excitonic features of the absorption edge are well accounted for within the model presented here. However, there are *additional* structures in the measured absorption profiles.

A relatively broad peak is observed about 7 meV above the exciton peak. We believe that this second peak in our absorption spectra is originating from built-in inhomogeneous stress that partly lifts the degeneracy of the heavy- and light-hole valence bands.²⁷ The internal stress apparently is difficult to avoid for the small and very thin samples used in this experiment. This interpretation of the second peak is supported by a number of observations: The intensity of the second peak varies with pressure like that of the main exciton. The energy separation between the two peaks remains constant up to ~ 5 GPa and then increases slightly with pressure (at 8 GPa the separation amounts to about 12 meV). This indicates that He is no longer fully hydrostatic above 5 GPa. We have observed a similar but more intense structure in absorption spectra when Xe was used as the pressure-transmitting medium, which has a larger shear strength compared to He. Finally, Sturge¹¹ also reported the appearance of double-exciton peaks for stressed GaAs samples at low temperatures.

Absorption spectra measured at 100 and 20 K show an *additional shoulder* at the low-energy side of the exciton peak, which increases in intensity when pressure is raised up to the crossover pressure P_c . At 100 K and 4.5 GPa the shoulder develops into a clearly resolved peak 3 meV below the exciton line. For higher pressures this additional shoulder or peak always disappears (at 6 GPa it is no longer observable). An optical transition situated a few meV below the $1s$ exciton line has also been observed in the absorption spectra of very pure epitaxial GaAs

samples.¹ It has been associated with transitions to excitonic states bound to neutral donors, which can have a giant oscillator strength²⁸ with enhancement factors of the order of 10^6 . Furthermore, luminescence experiments on GaAs under pressure²⁹ demonstrate that below the Γ - X crossover the energy of shallow donor levels follows the blue shift of the E_0 fundamental gap. Above the band crossing donors couple to the lower-lying X -point conduction-band minimum. According to these observations, we associate the low-energy shoulder or peak with bound-exciton optical absorption.

In the fitting of Eq. (7) to the measured optical-absorption spectra (see solid lines in Fig. 2) we have neglected data points in those spectral regions where the additional structures occur. In this way we ensure satisfactory fits of the main exciton peak and the absorption coefficient in the exciton continuum regime. From the results of these fits we determine the pressure dependence of the E_0 energy gap and of exciton parameters.

B. The E_0 band gap and absorption strength C_0

The energy E_0 of the direct band gap is given by $E_0 = E_{1s} + \mathcal{R}$. The pressure dependence of E_0 at 200 and 100 K is shown in Fig. 4. A similar result is obtained for $T=20$ K. The linear and quadratic pressure coefficients of E_0 are listed in Table I together with other experimental results at 300 K (Ref. 17) and 4 K.²⁹ Our values of E_0 at normal pressure agree with those determined by ellipsometry.³⁰ We note that the pressure coefficients of the E_0 fundamental gap of GaAs are, within experimental error, independent of temperature.

The parameter C_0 [Eq. (5)] determines the strength of the exciton absorption as predicted by Elliott's theory. Within $\mathbf{k}\cdot\mathbf{p}$ theory the reduced effective mass μ at the Γ point is proportional to the direct-band-gap energy E_0 .³¹

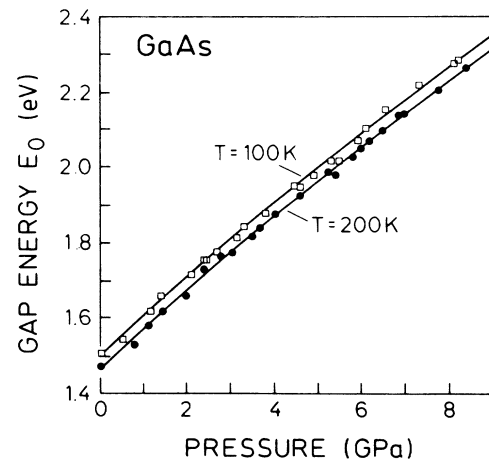


FIG. 4. Energy E_0 of the direct band gap of GaAs at 200 and 100 K as a function of pressure. First- and second-order pressure coefficients corresponding to the solid lines are given in Table I.

TABLE I. First- and second-order pressure coefficients of the direct optical gap E_0 of GaAs [$E_0(P) = E_0(P=0) + bP + cP^2$] at different temperatures. Experimental results for other temperatures are also given for comparison.

T (K)	$E_0(P=0)$ (eV)	b (10^{-2} eV/GPa)	c (10^{-4} eV/GPa ²)
300	1.43(1) ^a	10.8(3) ^a	-14(2) ^a
200	1.465(6)	10.6(3)	-13(4)
100	1.505(6)	10.6(4)	-16(7)
20	1.512(6)	10.7(4)	-14(5)
4	1.5192(2) ^b	10.73(5) ^c	

^aReference 17.

^bReference 1.

^cReference 29.

One thus expects that $C_0 \sim E_0^{3/2}$. The values of C_0 for 200 K, when plotted versus $E_0^{3/2}$, lie on a straight line, as shown in Fig. 5. The same behavior is found for the C_0 data at 100 and 20 K. This, in fact, implies that the matrix element M_R of the electron-photon interaction for dipole-allowed transitions, which is given by the interband momentum operator $P \sim 2\pi/a$, is essentially independent of pressure. One can obviously neglect the small variation with pressure of the lattice parameter a compared to the change of E_0 .

A roughly linear increase of the absorption coefficient $\alpha(E_0)$ at the direct edge was reported for GaAs (Ref. 17) and Ge (Ref. 32) at $T=300$ K. This effect was attributed to exciton formation. The present results obtained at low temperatures confirm this dependence of the absorption coefficient on the gap energy, since according to Eqs. (2), (5), and (7) one has $\alpha(E_0) \sim C_0 \mathcal{R}^{1/2} / E_0 \sim E_0$. Contributions to the absorption coming from indirect transitions to the lower-lying X -point conduction-band minimum ($P > 4.2$ GPa) are negligible in the pressure range investigated here.

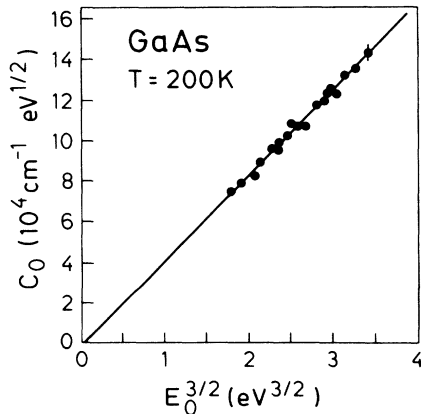


FIG. 5. The absorption-strength parameter C_0 as defined in Eq. (5) vs energy gap E_0 for measurements at 200 K. The solid line is a fit to the data with a linear function.

C. Exciton binding energy

Figure 6 shows the exciton binding energy \mathcal{R} as a function of pressure for three different temperatures. The solid lines in Fig. 6 represent the results of fitting a linear function to the data points. The corresponding values of \mathcal{R} extrapolated to zero pressure and the slopes are given in Table II together with other experimental and theoretical results. The values of \mathcal{R} at 200 K determined here is in good agreement with that in Ref. 1, where \mathcal{R} was deduced from the energy difference between the $m=1$ and 2 exciton-absorption lines.

The validity of the description of the E_0 exciton of GaAs in terms of a hydrogenic model is not obvious because of the degeneracy of the light- and heavy-hole bands. Equation (2) can nevertheless be used to estimate the effective rydberg energy \mathcal{R} , provided that an average value μ for the reduced mass is introduced as given by⁷

$$\mu^{-1} = m_e^{-1} + (m_{lh}^{-1} + m_{hh}^{-1})/2. \quad (8)$$

Here m_e is the electron conduction-band mass and m_{lh} (m_{hh}) are the light- (heavy-) hole valence-band effective masses. By using the data for GaAs from Ref. 35 ($m_e/m_0 = 0.068$, $m_{lh}/m_0 = 0.076$, $m_{hh}/m_0 = 0.5$, and $\epsilon = 12.5$) one finds from Eq. (2) a value for \mathcal{R} that is only 10% smaller than the experimental value at 2 K of Ref. 1 (see Table II). Actually, the binding energy can be calculated more accurately. Baldereschi and Lipari⁷ have developed a perturbation method that allows to calculate the energy position of the 1s and the 2s levels of the fourfold-degenerate E_0 exciton in tetrahedral semiconductors. In the case of GaAs, they find excellent agreement (within 1%) of their calculated binding energy with the experimental one.

At all temperatures we observe an essentially linear increase of the exciton effective rydberg (see Fig. 6). Actually, the simple hydrogenic model predicts, to a first approximation, a linear pressure dependence for \mathcal{R} in GaAs [see Eq. (2)]: The static dielectric constant ϵ of GaAs

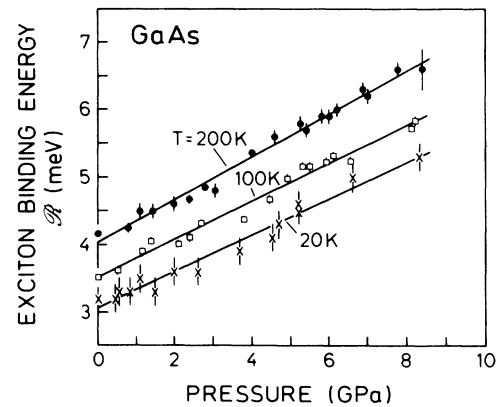


FIG. 6. Exciton binding energy \mathcal{R} of GaAs at 200, 100, and 20 K as a function of pressure. The lines are fits to the data with linear expressions (corresponding parameters are listed in Table II).

TABLE II. Binding energy \mathcal{R} and its pressure coefficient of the direct exciton of GaAs at different temperatures. Other experimental and theoretical results are given for comparison.

T (K)	\mathcal{R} (meV)		$d \ln \mathcal{R} / dP$ (GPa $^{-1}$)
	Experiment	Theory	
200	4.0(1) ^a		0.083(3) ^a
	3.0(4) ^b		
100	3.5(1) ^a		0.080(3) ^a
	3.3(5) ^b		
20	3.1(1) ^a		0.086(3) ^a
	3.4(5) ^b		
2	4.2(2) ^c		
	4.4 ^d		
		3.9 ^e	
		4.1 ^f	
		4.22 ^g	

^aThis work, absorption (fit).

^bReference 11, absorption (fit).

^cReference 1, absorption (energy difference of $m = 1, 2$ lines).

^dReference 33, luminescence.

^eFrom Eqs. (2) and (9), H-atom model.

^fReference 7, perturbation theory.

^gReference 34, variational calculations.

does not change appreciably with pressure.³⁶ Thus, the exciton effective rydberg \mathcal{R} is proportional to the reduced mass μ (within $\mathbf{k} \cdot \mathbf{p}$ theory³¹ we have $\mu \propto E_0$), i.e., $\mathcal{R} \propto E_0$.

The E_0 fundamental gap increases by only 3% between 200 and 20 K. Furthermore, from the analysis of absorption spectra Sturge¹¹ deduced no substantial change of \mathcal{R} with decreasing temperature (see Table II). However, we find the parameter \mathcal{R} to decrease by 25% in the same temperature range. In our case we cannot completely rule out that the additional structure found in the absorption spectra at energies above the main exciton peak (discussed in Sec. III A) has some influence on the determination of \mathcal{R} , because these structures become more pronounced at low temperature (see Fig. 2). However, we offer a physical explanation for this effect in terms of an increase of the low-frequency dielectric constant ϵ at low temperatures.

A strong enhancement of the electronic polarizability occurs when the concentration of neutral donors approaches some critical value for the insulator-metal transition.³⁷ In Si:As (Ref. 38) a significant increase of ϵ has been observed for donor concentrations close to $6 \times 10^{18} \text{ cm}^{-3}$ when the donors are not thermally ionized. Furthermore, Castner³⁷ estimated for Si a 10% increase of ϵ for concentrations between 5×10^{17} and 10^{18} cm^{-3} (which corresponds to a 20% decrease of \mathcal{R}). The Mott transition in GaAs is expected at donor concentrations approximately 2 orders of magnitude lower than in Si, due to the smaller conduction-band mass in GaAs, i.e., larger donor-effective Bohr radius. Donor concentrations of 10^{16} cm^{-3} are common for a semi-insulating GaAs wafer^{11,39} as used in the present experiment. Therefore, the main effect contributing to the decrease of \mathcal{R} with decreasing temperature may well be related to an increase of ϵ due to the freeze out of carriers at shallow donor

states. This interpretation, which is supported by the fact that $d \ln \mathcal{R} / dP$ is approximately constant and independent of temperature (see Table II), deserves further study.

D. Exciton line broadening above the Γ -X crossover

The values of the half-width Γ_1 of the $1s$ exciton line as a function of pressure are shown in Fig. 7 for the three different temperatures. At normal pressure Γ_1 is reduced by 50%, when temperature changes from 200 to 20 K. The interaction of excitons with impurities or defects depends on the quality of the sample and yields a roughly temperature-independent exciton linewidth (for undoped materials). Thus, the strong temperature dependence of the exciton linewidth indicates that electron-phonon interaction is a dominant scattering mechanism in our samples.

The width Γ_1 remains approximately constant up to the Γ -X crossover pressure P_c . For $P > P_c$ the exciton line broadens significantly (see Fig. 7), this broadening being stronger for higher temperatures. Obviously the data in Fig. 7 allow one to distinguish two pressure ranges below and above P_c characterized by different excitonic scattering mechanisms.

In the pressure range below P_c excitons can be scattered within the conduction-band minimum at point Γ by phonons with small wave vectors \mathbf{q} . Toyozawa²⁴ has shown that the strength of the exciton-phonon coupling via *deformation-potential* interaction is proportional to q in the case of the optic modes, but proportional to $q^{1/2}$ for acoustic ones. For that reason acoustic phonons are mainly responsible for *intravalley* scattering. The scattering times⁴⁰ are inversely proportional to the phonon occupation number $N_q = [\exp(E_q/k_B T) - 1]^{-1}$. The aver-

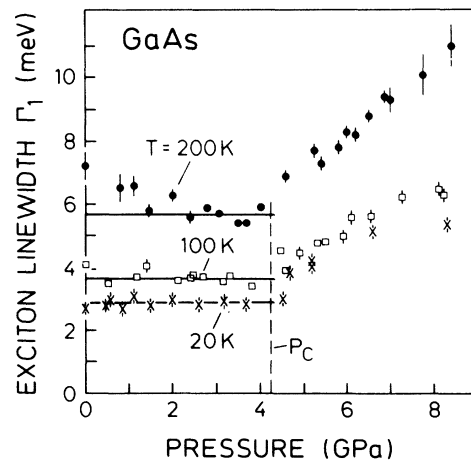


FIG. 7. Half-width Γ_1 of the direct exciton peak of GaAs at 200, 100, and 20 K as a function of pressure. Horizontal lines represent the mean width for pressures below the critical pressure P_c for Γ -X crossover. For 200 K only data points for pressures close to P_c were considered for the average.

age values of Γ_1 for $P < P_c$ (see horizontal lines in Fig. 7) at different temperatures follow well that behavior with an average phonon frequency $E_q \sim 17$ meV (for $T=200$ K only data points for $2 \text{ GPa} < P < P_c$ were considered in evaluating the average width).

For $P > P_c$ phonon-assisted *intervalley* scattering of electrons from Γ - to X -point conduction-band states becomes possible. Now both acoustic- and optical-phonon modes contribute to the scattering probability. We thus attribute the corresponding decrease of the exciton lifetime for $P > P_c$ to phonon-assisted transitions from the Γ - to the X -point conduction-band valleys. From the broadening effect we can evaluate the phonon deformation-potential constant for intervalley scattering in GaAs.

We define the broadening $\Delta\Gamma$ for a given pressure P greater than P_c as the difference between the actual linewidth Γ_1 and the average width below P_c given by the horizontal lines in Fig. 7. The $\Delta\Gamma$ data obtained in this way are shown in Fig. 8 as a function of the energy difference $\Delta E_{\Gamma X}$ between the Γ and the X points in the conduction band. The energy difference $\Delta E_{\Gamma X}$ is calculated for different pressures using the direct-band-gap pressure coefficients obtained in the present work and the indirect Γ - X gap pressure coefficient after Ref. 17. The broadening $\Delta\Gamma$ is more pronounced at 200 K than at lower temperatures, as is clearly shown by the data of Fig. 8.

To interpret the exciton-broadening data we have used a simple model for intervalley electron scattering within the effective-mass approximation.⁴¹ As a scattering mechanism the phonon-induced deformation potential is

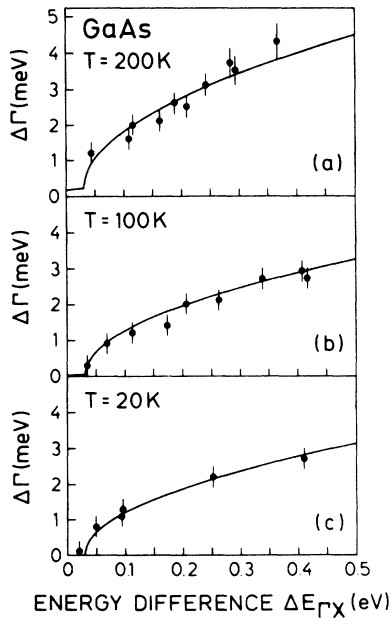


FIG. 8. Broadening $\Delta\Gamma$ of the direct exciton of GaAs for pressures greater than P_c , (a) at 200 K, (b) at 100 K, and (c) at 20 K as a function of the conduction-band energy difference $\Delta E_{\Gamma X}$. Solid curves are the results of fitting Eq. (10) to the experimental data with S as the only adjustable parameter.

considered. The corresponding matrix element is given by⁴²

$$|M_S| = \left[\frac{\hbar^2}{2\rho E_q} \right]^{1/2} D_{\Gamma X} \sqrt{N_q + \frac{1}{2} \pm \frac{1}{2}}, \quad (9)$$

where E_q and N_q are the phonon energy and occupation number, respectively, of a given phonon with wave vector \mathbf{q} , ρ is the material density, and $D_{\Gamma X}$ is the phonon deformation-potential constant for Γ - X intervalley scattering (in units of eV/Å). The possible dispersion of $D_{\Gamma X}$ is neglected here. The plus (minus) sign in Eq. (9) corresponds to the emission (absorption) of a phonon. By symmetry only certain phonon modes can participate in the scattering process. In GaAs the first conduction band at the X point has X_1 symmetry.⁴³ Thus only zone-edge LO phonons⁴⁴ mediate electronic transitions from point Γ to point X . We take $E_q \approx 30$ meV for the energy of the LO phonons at the X point of GaAs.¹⁹

The exciton broadening induced by scattering with phonons is simply related to the transition probability through Fermi's golden rule. Considering a parabolic conduction-band dispersion at the Γ and X points, the broadening $\Delta\Gamma$ is expressed as a function of the energy difference $\Delta E_{\Gamma X}$ as⁴¹

$$\Delta\Gamma(\Delta E_{\Gamma X}) = \frac{S}{E_q} [f_B(T) \sqrt{\Delta E_{\Gamma X} - E_q} + \sqrt{\Delta E_{\Gamma X} + E_q}] \quad (10)$$

with

$$S = \frac{3m_x^{3/2} D_{\Gamma X}^2}{2\sqrt{2}\pi\hbar\rho} N_q(T). \quad (11)$$

Here $f_B = \exp(E_q/k_B T)$ is the Boltzmann factor, $\rho = 5.34(2) \text{ g/cm}^3$ for GaAs,¹⁹ and $m_x = (m_{\Gamma}^2 m_{\parallel})^{1/3} = 0.43$ is the density-of-states effective mass at the X -point conduction-band minimum.⁴⁵

The solid curves in Fig. 8 are obtained by fitting Eq. (10) to the experimental broadening $\Delta\Gamma$ at the three selected temperatures. The factor S is the only adjustable parameter. Its values obtained in this manner allow us to determine the deformation potential (i.e., the electron-phonon coupling constant) $D_{\Gamma X}$ for Γ - X interband electron-LO-phonon interaction of GaAs. We have obtained for $D_{\Gamma X}$ at 200, 100, and 20 K the values 4.9(5), 4.8(4), and 4.8(4) eV/Å, respectively. In accordance with Ref. 44, $D_{\Gamma X}$ is found to be independent of temperature. We take the mean value as the final result, i.e.,

$$D_{\Gamma X} = 4.8(3) \text{ eV/Å}.$$

Scattering deformation potentials were usually derived indirectly from high-field transport experiments (i.e., microwave oscillations) or by measuring relaxation times of field-excited or photoexcited carriers. The disadvantage of these methods is that the interpretation of the experimental results is not straightforward, because information about the scattering mechanism is obtained through complicated Monte Carlo simulations of the transport properties.^{45,46} Values for $D_{\Gamma X}$ obtained with these

methods lie in the range 5–10 eV/Å. The $D_{\Gamma X}$'s were also calculated using rigid-ion empirical pseudopotential methods^{44,47} giving $D_{\Gamma X} \approx 3$ eV/Å, in reasonable agreement with the present experimental value. The agreement may improve if *ab initio*, self-consistent calculations are performed.

IV. CONCLUSIONS

We summarize the results of low-temperature exciton-absorption studies of GaAs under high hydrostatic pressure as follows. (1) The energy of the direct band gap E_0 of GaAs exhibits a sublinear dependence on pressure with a linear coefficient of 0.107(4) eV/GPa. Within experimental error the linear and quadratic pressure coefficients are independent of temperature and consistent with literature data.^{17,29} (2) The strength of the absorption coefficient $\alpha(E_0)$ at the direct optical gap energy increases with pressure and is proportional to the energy of the E_0 fundamental gap. This result is consistent with Elliott's theory of exciton absorption.^{10,17} (3) The binding energy \mathcal{R} of the direct exciton in GaAs increases linearly with pressure. The average slope in the temperature range 20–200 K is $d \ln \mathcal{R} / dP = 0.083(3)$ GPa⁻¹. This pressure dependence of \mathcal{R} can be understood as being due to an increase of the reduced effective mass of the exciton with pressure.³¹ (4) The exciton linewidth in GaAs, which remains essentially constant up to the Γ - X crossover pressure P_c , broadens significantly above this pressure due to phonon-assisted intervalley scattering processes. From this broadening we determine the phonon deformation potential $D_{\Gamma X}$ for Γ - X intervalley scattering in GaAs. Our result for $D_{\Gamma X}$ is probably the first reliable determination of this quantity.

ACKNOWLEDGMENTS

We thank K. Reimann for helpful discussions. We gratefully acknowledge technical assistance by W. Böhringer, W. Dieterich, and S. Heymann. We also

thank A. Böhringer for preparation of the samples. One of the authors (A.C.) wishes to thank the Ministerio de Educación y Ciencia of Spain for financial support.

APPENDIX

Rewriting the exponential function in the integrand of Eq. (3a) as

$$\frac{1}{1 - e^{-2\pi z}} = \frac{1}{2} [1 + \coth(\pi z)],$$

the contribution to the absorption coefficient coming from transitions into the exciton continuum splits into two integrals:

$$\begin{aligned} I_c &= I_{c1} + I_{c2} \\ &= \frac{1}{2} \int_{E_0}^{\infty} dE \frac{\Gamma_c}{(E - \hbar\omega)^2 + \Gamma_c^2} \\ &\quad + \frac{\Gamma_c}{2} \int_{E_0}^{\infty} dE \frac{\coth(\pi z)}{(E - \hbar\omega)^2 + \Gamma_c^2}. \end{aligned} \quad (\text{A1})$$

I_{c1} can be directly integrated, giving

$$I_{c1} = \frac{\pi}{4} - \frac{1}{2} \arctan \left[\frac{E_0 - \hbar\omega}{\Gamma_c} \right]. \quad (\text{A2})$$

The integral I_{c2} can be solved in the complex plane with the following substitution of variables:

$$x^2 = z^{-2} = (E - E_0)/\mathcal{R}; \quad \xi^2 = (E_0 - \hbar\omega)/\mathcal{R}; \quad \gamma_c = \Gamma_c/\mathcal{R}.$$

This gives for I_{c2}

$$I_{c2} = \gamma_c \int_0^{\infty} dx \frac{x}{(x^2 + \xi^2)^2 + \gamma_c^2} \coth \left[\frac{\pi}{x} \right]. \quad (\text{A3})$$

The poles of the integrand in the upper hemisphere of the complex plane are

$$\left. \begin{aligned} x_1 &= (-\xi^2 + i\gamma_c)^{1/2} \\ x_2 &= -(-\xi^2 - i\gamma_c)^{1/2} \end{aligned} \right\} \text{in the denominator of Eq. (A3);}$$

$$x_m = \frac{i}{m}, \quad m = 1, 2, 3, \dots \text{ in } \coth(\pi/x).$$

By integrating Eq. (A3) along the real axis and a half-circle in the upper half-plane one thus obtains

$$I_{c2} = \frac{\pi}{4} \left[\coth \left[\frac{\pi}{(-\xi^2 + i\gamma_c)^{1/2}} \right] + \coth \left[\frac{\pi}{(-\xi^2 - i\gamma_c)^{1/2}} \right] \right] - \gamma_c \sum_{m=1}^{\infty} \frac{1}{m^3} \frac{1}{(\xi^2 - 1/m^2)^2 + \gamma_c^2}. \quad (\text{A4})$$

The final result of Eq. (7) is obtained from Eq. (A4) by taking $u_1 = \pi/x_1 = u^+ + iu^-$ and $u_2 = u_1^*$ (complex conjugate):

$$I_{c2} = \frac{\pi}{2} \frac{\sinh(2u^+)}{\cosh(2u^+) - \cos(2u^-)} - \sum_{m=1}^{\infty} \frac{\mathcal{R}}{m^3} \frac{\Gamma_c}{(\hbar\omega - E_m)^2 + \Gamma_c^2}. \quad (\text{A5})$$

We note that I_{c2} is a monotonic function of photon energy (it can be demonstrated that it is related to the Φ function, i.e., the logarithmic derivative of the Γ function).

- *On leave from Facultat de Física, Universitat de València, Burjassot, E-46100 València, Spain.
- ¹D. D. Sell, Phys. Rev. B **6**, 3750 (1972).
- ²J. I. Pankove, *Optical Processes in Semiconductors* (Dover, New York, 1975).
- ³P. J. Dean and D. C. Herbert, in *Bound Excitons in Semiconductors*, Vol. 14 of *Topics in Current Physics*, edited by K. Cho (Springer, Berlin, 1979), p. 55.
- ⁴E. I. Rashba and M. D. Sturge, in *Excitons*, Vol. 2 of *Modern Problems in Condensed Matter Science*, edited by V. M. Agranovich and A. A. Maradudin (North-Holland, Amsterdam, 1982).
- ⁵T. Takizawa, J. Phys. Soc. Jpn. **52**, 1057 (1983).
- ⁶R. J. Elliott, *Theory of Excitons I*, in *Polarons and Excitons*, edited by C. G. Kuper and G. D. Whitfield (Oliver and Boyd, Edinburgh, 1963).
- ⁷A. Baldereschi and N. C. Lipari, Phys. Rev. B **3**, 439 (1971).
- ⁸E. O. Kane, Phys. Rev. B **11**, 3850 (1975).
- ⁹M. Altarelli and N. O. Lipari, in *Theory of Excitons in Semiconductors*, Proceedings of the 13th International Conference on the Physics of Semiconductors, Rome, 1976, edited by F. G. Fumi (North-Holland, Amsterdam, 1977).
- ¹⁰R. J. Elliott, Phys. Rev. **108**, 1384 (1957).
- ¹¹M. D. Sturge, Phys. Rev. **127**, 768 (1962).
- ¹²S. Ves and M. Cardona, Solid State Commun. **38**, 1109 (1981).
- ¹³N. Kuroda, O. Ueno, and Y. Nishina, J. Phys. Soc. Jpn. **55**, 581 (1986).
- ¹⁴N. Kuroda, O. Ueno, and Y. Nishina, Phys. Rev. B **35**, 3860 (1987).
- ¹⁵M. Gauthier, A. Polian, J. M. Besson, and A. Chevy, Phys. Rev. B **40**, 3837 (1989).
- ¹⁶K. Reimann and K. Syassen, Phys. Rev. B **39**, 11 113 (1989).
- ¹⁷A. R. Goñi, K. Strössner, K. Syassen, and M. Cardona, Phys. Rev. B **36**, 1581 (1987), and references therein.
- ¹⁸A. R. Goñi, A. Cantarero, K. Syassen, and M. Cardona, High Pressure Res. (to be published).
- ¹⁹*Numerical Data and Functional Relationships in Science and Technology*, Vol. 17a of *Landolt-Börnstein*, New Series, edited by O. Madelung, H. Weiss, and M. Schulz (Springer, Heidelberg, 1982).
- ²⁰J. D. Barnett, S. Block, and G. J. Piermarini, Rev. Sci. Instrum. **44**, 1 (1973).
- ²¹H. K. Mao, J. Xu, and P. M. Bell, J. Geophys. Res. **91**, 4673 (1986).
- ²²D. M. Adams, R. Appleby, and S. K. Sharma, J. Phys. E **9**, 1140 (1976).
- ²³R. A. Noack and W. B. Holzapfel, in *High Pressure Science and Technology*, edited by K. D. Timmerhaus and M. S. Barber (Plenum, New York, 1979), Vol. 1, p. 748.
- ²⁴Y. Toyozawa, Prog. Theor. Phys. **20**, 53 (1958).
- ²⁵D. D. Sell and P. Lawaetz, Phys. Rev. Lett. **26**, 311 (1971).
- ²⁶R. Le Toullec, N. Piccioli, and J. C. Chervin, Phys. Rev. B **22**, 6162 (1980).
- ²⁷F. H. Pollak and M. Cardona, Phys. Rev. **172**, 816 (1968).
- ²⁸C. H. Henry and K. Nassau, Phys. Rev. B **1**, 1628 (1970).
- ²⁹D. J. Wolford and J. A. Bradley, Solid State Commun. **53**, 1069 (1985).
- ³⁰P. Lautenschlager, M. Garriga, S. Logothetidis, and M. Cardona, Phys. Rev. B **35**, 9174 (1987).
- ³¹M. Cardona, in *Atomic Structure and Properties of Solids*, edited by E. Burstein (Academic, New York, 1972).
- ³²A. R. Goñi, K. Syassen, and M. Cardona, Phys. Rev. B **39**, 12 921 (1989).
- ³³M. A. Gilleo, P. T. Bailey, and D. E. Hill, J. Lumin. **1/2**, 562 (1970).
- ³⁴Y. Abe, J. Phys. Soc. Jpn. **19**, 818 (1964).
- ³⁵S. Adachi, J. Appl. Phys. **58**, R1 (1985).
- ³⁶A. R. Goñi, K. Syassen, K. Strössner, and M. Cardona, Semicond. Sci. Technol. **4**, 246 (1989), and unpublished results.
- ³⁷T. G. Castner, Phys. Rev. B **21**, 3523 (1980).
- ³⁸T. G. Castner, N. K. Lee, G. S. Cieloszyk, and G. L. Salinger, Phys. Rev. Lett. **34**, 1627 (1975).
- ³⁹E. Bauser (private communication).
- ⁴⁰K. Seeger, *Semiconductor Physics. An Introduction* (Springer, Heidelberg, 1985).
- ⁴¹E. M. Conwell, *High Field Transport in Semiconductors* (Academic, New York, 1967).
- ⁴²O. Madelung, *Introduction to Solid-State Theory* (Springer, Heidelberg, 1982).
- ⁴³R. Wentzcovitch, M. Cardona, M. L. Cohen, and N. E. Christensen, Solid State Commun. **67**, 927 (1988).
- ⁴⁴S. Zollner, S. Gopalan, and M. Cardona, Appl. Phys. Lett. (to be published).
- ⁴⁵K. F. Brennan, D. H. Park, K. Hess, and M. A. Littlejohn, J. Appl. Phys. **63**, 5004 (1988).
- ⁴⁶M. V. Fischetti and S. E. Laux, Phys. Rev. B **38**, 9721 (1988).
- ⁴⁷D. C. Herbert, J. Phys. C **6**, 2788 (1974).